Electromechanical study of polyurethane films with carbon black nanoparticles for MEMS actuators

OPEN ACCESS
IOP Publishing
Journal of Micromechanics and Microengineering
J. Micromech. Microeng. **24** (2014) 055011 (8pp)
doi:10.1088/0960-1317/24/5/055011

Electromechanical study of polyurethane films with carbon black nanoparticles for MEMS actuators

M Roussel[1], C Malhaire[2], A-L Deman[1], J-F Chateaux[1], L Petit[3], L Seveyrat[3], J Galineau[3], B Guiffard[4], C Seguineau[5], J-M Desmarres[6] and J Martegoutte[6]

[1] Université de Lyon, Institut des Nanotechnologies de Lyon INL-UMR5270, CNRS, Université Lyon 1, Villeurbanne, F-69622, France
[2] Université de Lyon, Institut des Nanotechnologies de Lyon INL-UMR5270, CNRS, INSA de Lyon, 7 av. Jean Capelle, bât. Blaise Pascal, Villeurbanne, F-69621, France
[3] LGEF, INSA-Lyon, 8 rue de la Physique, F-69621, Lyon, France
[4] Lunam Université, IETR UMR CNRS 6164, Université de Nantes, 2 rue de la Houssinière, BP 92208, F-44322 Nantes Cedex 3, France
[5] Fialab, CNES, DCT/AQ/LE bpi 1414, 18 avenue Édouard Belin, Toulouse Cedex 9, F-31401, France
[6] CNES, DCT/AQ/LE bpi 1414, 18 avenue Édouard Belin, Toulouse Cedex 9, F-31401, France

E-mail: christophe.malhaire@insa-lyon.fr

Received 10 September 2013, revised 14 November 2013
Accepted for publication 17 December 2013
Published 11 April 2014

Abstract

Pure polyurethane and nanocomposite carbon black (CB) polyurethane solutions were deposited by spin-coating on a silicon substrate using gold as the adhesion layer and electrode. Different test structures were achieved for electrical and mechanical characterizations. The incorporation of CB nanoparticles in the polyurethane matrix has a significant influence on the dielectric permittivity of the material with an increase of about one third of its value. The Young's modulus of PU and nanocomposite PU films was determined by different characterization methods. Nanoindentation experiments have pointed out a Young's modulus gradient through the film thickness. By performing mechanical tests (tensile, bulge, point deflection) on freestanding films, an average Young's modulus value of about 30 MPa was found as well as a residual stress value of about 0.4 MPa. However, no influence of the presence of the nanoparticles was found. Finally, several MEMS actuators were realized and characterized. At their fundamental resonance frequency, the actuation of the nanocomposite membranes is more efficient than that of pure polyurethane. However, the time constant of the material seems to provide a major barrier for the development of high-frequency PU-based micro-actuators.

Keywords: MEMS, actuator, polyurethane, carbon black, electrostriction

1. Introduction

Electroactive polymer (EAP) transducers are an emerging technology that offers great opportunities for the development of actuators [1–3]. Among them, dielectric EAP for actuators (DEAs) have some advantages over some traditional electroactive materials such as electro-ceramics or magnetostrictive materials due to their high strain, flexibility, low energy consumption and low cost [4]. DEA actuation is driven by electric field or Coulomb force. They can be used to develop thin film-based actuators that consist of a polymer film sandwiched between two compliant electrodes. Two mechanisms contribute to the actuation phenomenon: Maxwell's effect and the true electrostrictive effect [3, 5]. Maxwell stress is a result of the electrostatic interaction between oppositely charged electrodes. The

negative deformation (compression) between electrodes in the direction of the electric field is

$$S_{\mathrm{Max}} = -\varepsilon_0 \varepsilon_r \frac{E^2}{2Y}, \tag{1}$$

where Y is the Young's modulus, E the applied electric field, ε_r is the real part of the dielectric constant and ε_0, the vacuum dielectric permittivity. True electrostriction is due to the reorientation and mutual attraction under an applied electric field of induced or permanent dipoles present in the dielectric. This microscopic movement induces macroscopic deformation in the polymer:

$$S_E = -Q\varepsilon_0^2(\varepsilon_r - 1)^2 E^2, \tag{2}$$

where Q (negative) represents the coefficient of true electrostriction. The total deformation of the electrostrictive polymer under an electric field is

$$S_{\mathrm{tot}} = S_{\mathrm{Max}} + S_E = ME^2, \tag{3}$$

where M is the apparent electrostrictive coefficient in the direction of the electric field. All dielectric elastomers are subjected to both effects, however one mechanism may prevail over the other. In amorphous and low-polar elastomers, like polydimethylsiloxane (PDMS), Maxwell stress dominates electrostriction. However, polar elastomers, or semi-crystalline elastomers having numerous interfaces between nanodomains of different dielectric permittivity, true electrostriction can prevail [5]. Some types of polyurethane elastomers possess interesting electrostrictive properties, as they comprise soft segments [6], responsible for the elasticity of the polymer, and hard polar segments that orient themselves in the presence of an electric field [7]. Therefore, the electrostrictive effect is due to true electrostriction as well as the trapping of charges at the interfaces between soft and hard-segment domains. Several studies have compared the electro-mechanical properties of various types of polyurethane (PU) and demonstrated that true electrostriction is widely responsible for the electromechanical response of the material and the Maxwell stress is neglected [7, 8]. In addition, it was experimentally observed that Q is inversely proportional to the product of the Young's modulus and the dielectric permittivity [7]:

$$Q \propto \frac{1}{\varepsilon_0 \varepsilon_r Y}. \tag{4}$$

The apparent electrostrictive coefficient is then proportional to dielectric permittivity and inversely proportional to the Young's modulus (the assumption $\varepsilon_r \gg 1$ leads to simplification) [9]:

$$M \approx -Q\varepsilon_0^2(\varepsilon_r - 1)^2 \propto -\frac{1}{\varepsilon_0 \varepsilon_r Y}\varepsilon_0^2(\varepsilon_r - 1)^2 \rightarrow M \propto -\frac{\varepsilon_0 \varepsilon_r}{Y}. \tag{5}$$

An approach to improve the electromechanical response of an electrostrictive elastomer is to disperse conducting or semi-conducting nano-objects in the polymer matrix [9]. The goal is to increase the dielectric permittivity and to create nanodomains. Wongtimnoi *et al* [10] have shown that incorporation of carbon black in a PU matrix at a concentration of 1.25 vol% (in the vicinity of the percolation threshold) yields a threefold increase in the absolute value of the apparent electrostriction coefficient M at low frequency, compared to pure PU. Using nanoscale particles instead of larger ones, at low concentration, should not have a significant impact on the Young's modulus of the polymer; one objective of this study was to check this assumption.

Works dealing with the integration of electrostrictive elastomers in MEMS are not numerous in literature. Most of them are based on PDMS [11]. Indeed, PDMS possesses interesting processing properties such as soft-lithography and O_2 plasma surface activation, for optical [12] and fluidic applications [13]. However, electrostriction is dominated in PDMS by Maxwell stress and important electric fields are necessary to achieve significant deformation. As explained previously, PU elastomers and related composites present interesting electrostrictive properties but to our knowledge, there is no published work on its integration in MEMS. This study focuses on the electrical and mechanical characterization of pure and carbon black composite polyurethane films. The realization and the characterization of a first MEMS demonstrator are shown.

2. Pure and composite solution preparation

The polymer is a polyether-based thermoplastic PU, ref. Estane 58888 NAT021 Lubrizol. Hard segments comprise the 4.4' methylene bis(phenyl isocyanate) (MDI) and 1,4-butanediol (BDO) and soft segments are poly(tetramethylene oxide) (PTMO). The PU88 has a density of 1.13 g cm^{-3}, a hardness of 88 Shore A and the hard-segment content is about 46%. Carbon black (CB), Vulcan XC72R (Cabot Corp.), has a specific surface area of 254 m^2 g^{-1}. The primary CB nanoparticles have an average diameter of 30 nm and a specific gravity of 1.80. Pure and nanocomposite films were prepared from solutions. For pure solution, the granules were put in N,N-dimethylformamide (DMF, Sigma-Aldrich D158550, 99%): 20 wt% PU into DMF and mechanically stirred for 24 h up to complete dissolution.

In the case of the nanocomposite solution, the PU granules were heated at 80°C for 3 h before use. They were then put in N,N-dimethylformamide (DMF, Sigma-Aldrich D158550, 99%): 40 wt% PU into DMF. The solution was maintained at 80 °C for 2 h. At the same time, optimal CB volume fraction (1.25 vol% [10]) was dispersed in DMF using an ultrasonic processor (Hielsher UP400S, 400 W, 24 kHz, 7 mm diameter sonotrode) under the following experimental conditions: 20 min duration, 80% amplitude, 80% duty cycle. Subsequently, the two solutions were mixed together, heated and stirred until a homogeneous and viscous solution was obtained. This solution was degassed for 24 h at room temperature before use. Solutions were then spin coated on 4″ silicon wafer. The films were then placed on a hotplate at 115 °C for 15 min to remove the solvent.

3. Electrical characterizations

Capacitance measurements were done on test samples with a HP® 4284A impedance meter coupled to a probe station.

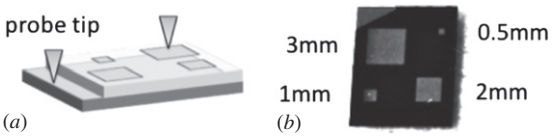

Figure 1. Permittivity measurements: (*a*) schematic drawing of a test sample, (*b*) picture of a composite CB+PU88 sample with top electrodes of different sizes.

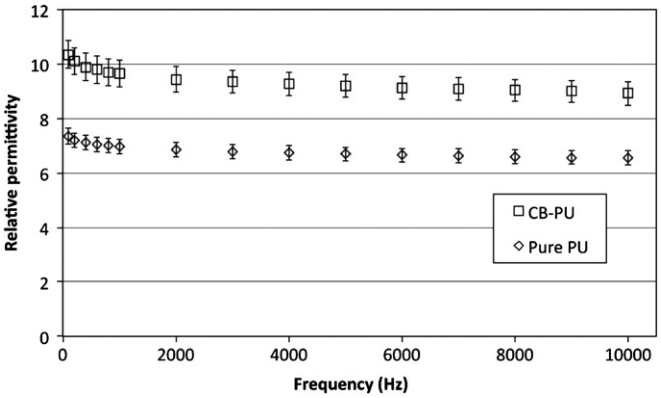

Figure 2. Relative permittivity as a function of the measurement frequency for different PU and CB+PU films.

PU solutions (20 wt%) were spin-coated (film thickness ranging from 19.2 to 25.1 μm) and baked (115 °C—15 min) on a 2″ silicon wafer previously metalized with Cr (10 nm) and Au (100 nm) layers. Top gold electrodes were evaporated through a shadow mask, to avoid any PU film damage which can occur with a photoresist-based process. Square shaped capacitors were achieved with the following side dimensions: 500 μm, 1 mm, 2 mm and 3 mm (figure 1). For each sample, the dielectric constant was determined from the slope of the capacitance (electrode surface) curve. A 2 V amplitude sinusoidal test signal was applied with a frequency ranging from 100 Hz to 10 kHz. Four pure PU and four composite PU samples were analyzed. The error bars in figure 2 take into account both the scatter between the data and the uncertainties in the determination of the dielectric constant. At 100 Hz, the composite dielectric constant is 1.41 times that of the pure one, reaching 10.4. At 10 kHz, the multiplication factor becomes 1.36 and the dielectric constant reaches 8.9 for composite PU. Using a parallel RC model, electrical conductivity was also determined. Conductivity of the composite PU (1.25 vol%) is very close to that of pure PU, ranging from 4.5×10^{-9} S m^{-1} at 100 Hz to 4×10^{-7} S m^{-1} at 10 kHz. The dissipation factor was between 0.04 and 0.07. All these data are in very good agreement with those already published in [10] and they confirm that the composite PU at 1.25 vol% concentration is just below the percolation threshold.

4. Mechanical characterizations

Several methods were employed to evaluate the Young's modulus and stress state of pure PU and nanocomposite PU films: nanoindentation measurements on films deposited on a thick substrate (surface mechanical characterization) and mechanical testing on free-standing polyurethane membranes (average in-plane elastic modulus and residual stress).

Table 1. Nanoindentation experiments: sample descriptions.

Sample	Nature	Thickness (μm)	Annealing
PU-1	PU88 pure	46	115 °C—15 min + 75 °C—5 h
PU-2	PU88 pure	46	115 °C—15 min + 60 °C—28 h
PU-3	PU88 composite	45	115 °C—15 min
PU-4	PU88 composite	45	115 °C—15 min + 75 °C—5 h

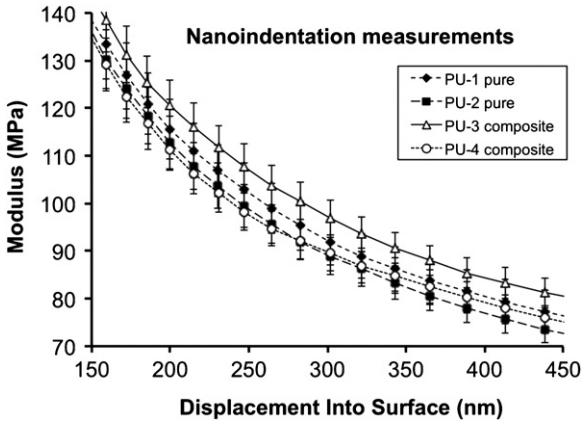

Figure 3. Young's modulus of pure and composite polyurethane coatings measured by nanoindentation.

4.1. Nanoindentation measurements

Nanoindentation experiments were performed on an Agilent® XP nanoindenter (dynamic contact module head). A CSM (continuous stiffness measurement) device was used for a continuous evaluation of the reduced modulus between 150 and 450 nm of indentation depth, in order to avoid substrate influence on the measurements, by following the Oliver and Pharr model [14]. A Poisson's ratio value of 0.49 was assumed. The characteristics of the four PU88 polyurethane coatings that were analyzed are summarized in table 1. For three samples, the short 115 °C—15 min annealing (after film deposition by spin-coating) was followed by a long annealing over several hours in order to simulate the thermal budget of the realization of a MEMS device (KOH etching of the silicon substrate to achieve membranes). For all samples, figure 3 shows a large variation of the Young's modulus as a function of the indentation depth, as for a layered solid. This phenomenon, previously reported by Wongtimnoi [15], is related to the film thickness and depends on the annealing conditions after film deposition. The hard-segment domain size may change through the film thickness as a function of the solvent evaporation kinetic. At the film surface, where rapid solvent evaporation favors hard and soft segment mixing, the hard-segment domain size is smaller than at the film/substrate interface leading to a larger density of cross-linking nodes, then a higher material stiffness. When considering measurement errors, carbon black nanoparticles do not seem to have any

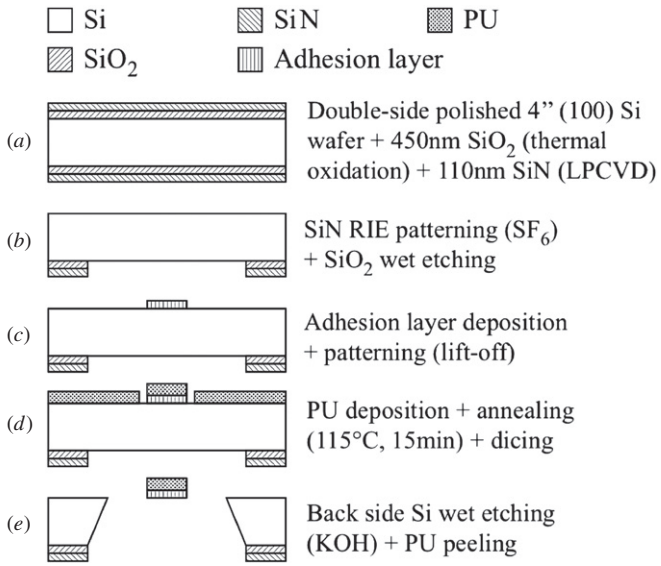

Figure 4. Process steps for the realization of PU tensile test specimens.

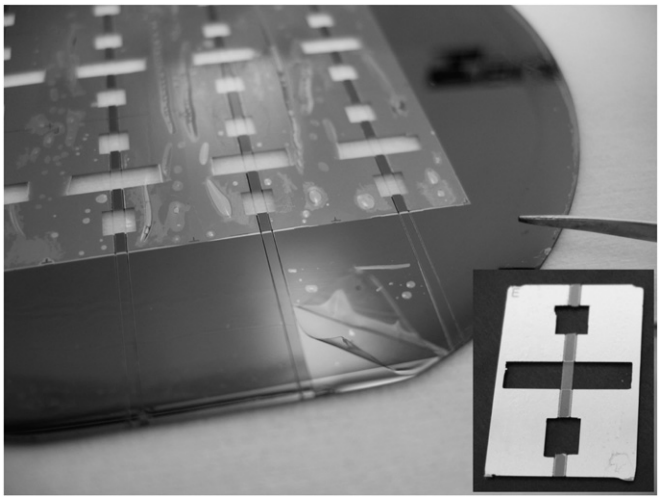

Figure 5. Picture of PU tensile test specimen fabrication: peeling off the polyurethane layer after the KOH etching process step (in insert: finished specimen).

significant influence on the modulus value. Presumably the concentration of CB nanoparticles on the first few hundred nanometers is not large enough to change the elasticity of the material.

4.2. Tensile tests

Micro-tensile experiments were performed on an experimental device already described elsewhere in [16, 17]. The main steps for the realization of polyurethane specimens are shown in figure 4 and pictures of a processed wafer and a finished specimen are shown in figure 5. As polyurethane film cannot be patterned, the beam geometry was defined by means of a dicing saw (Disco®). A thin film (about 50 nm) of Au/Cr was used as an adhesion layer before PU deposition (21 μm). This adhesion layer was patterned by lift-off in order to define anchor pads under the PU film. The pads were also used to

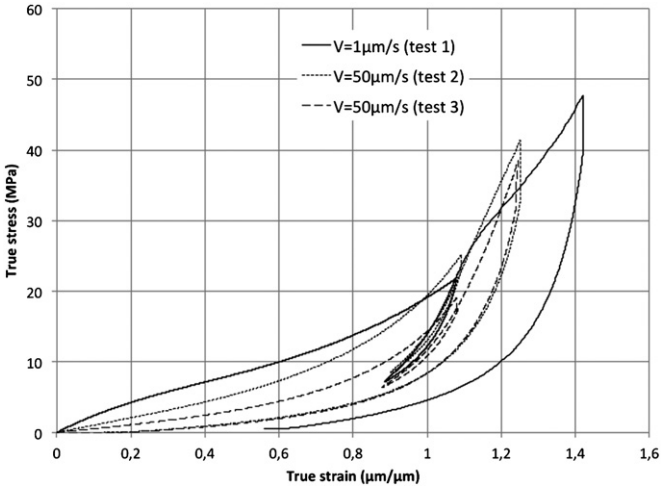

Figure 6. Stress–strain experimental curves for a 3 mm × 1 mm × 21 μm polyurethane specimen.

guide the dicing blade through the transparent polymer film. Unfortunately, that was not possible for composite films that were non-transparent and black in color. That is the reason why tensile tests were only performed on pure polyurethane films. After substrate etching, the excess PU film was peeled away from the substrate. Finally, the fixing holes of the specimens were released by hand using a cutting tool. The overall dimension (length × width × thickness) of each specimen was 20 mm × 14 mm × 450 μm whereas the PU beam (gage) dimension was 3 mm × 1 mm × 21 μm.

The obtained stress–strain experimental curves are given in figure 6. The displacement speed was set to 1 μm s^{-1} (first test) or 50 μm s^{-1} (second and third tests), and the applied stress remains uniaxial, allowing direct evaluation of the mechanical properties. During each measurement, a loop was performed at half cycle in order to observe any damage phenomenon. The change in the mechanical properties resulting from the first extension is clearly visible and is called Mullins' effect. From the beginning of the first curve, a Young's modulus value of (28.0 ± 0.7) MPa was calculated.

4.3. Measurements on free-standing membranes

4.3.1. Fabrication process of polyurethane membranes. Devices were achieved from thermally oxidized (1.5 μm) double-side polished (100) silicon wafers. On the back side, the oxide layer was used as masking layer for KOH etching of silicon. On the front side, SiO_2 played the role of an etching stop layer to protect PU or metallic layers. First, the back side SiO_2 was structured by photolithography and BOE etching in order to obtain square openings of 2 mm (figure 7(*a*)). On the front side, a Cr/Au (20 nm/40 nm) layer was deposited using an electron-gun evaporator and patterned by lift-off to achieve square openings aligned with those on the back side (figure 7(*b*)). The gold surface morphology was modified by *aqua regia* chemical etching (HCl (37%): HNO_3 (68%), 3:1, v:v) to improve PU adhesion. Indeed, we observed qualitatively a better adhesion of PU on Au with such a treatment than without any treatment. PU film was then

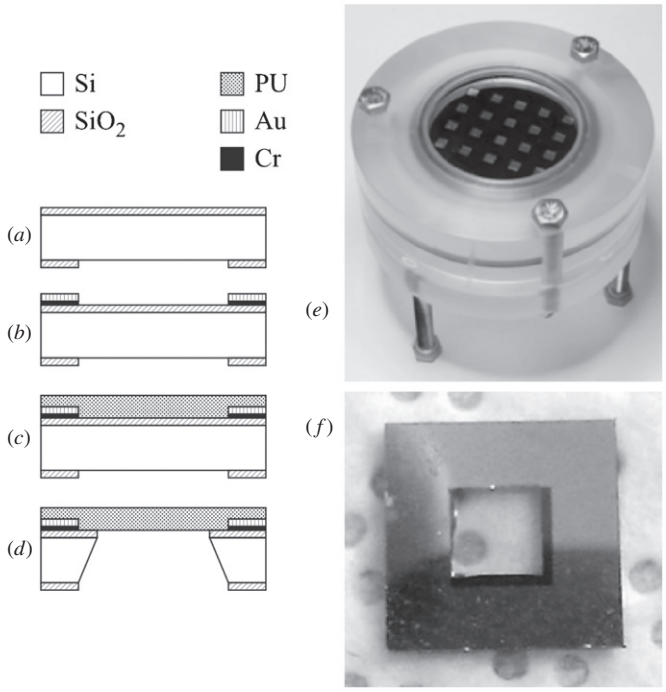

Figure 7. Process steps for the realization of polyurethane membranes.

deposited by spin-coating and baked on a hotplate at 115 °C for 15 min (figure 7(*c*)). In the last step, silicon was etched through SiO_2 square openings on the back side in a KOH solution heated at 80 °C, with an etch rate of 70 μm h^{-1}, in order to release the PU membrane (figure 7(*d*)). During this step, the silicon wafer was placed in a wafer holder designed to avoid any contact between the etching solution and the front side of the wafer. The volume between the wafer and the holder body was connected by a venting tube to the ambient atmosphere in order to balance the pressure on each side of the membrane and avoid any deformation of the polymer during the long duration time of silicon etching. A photograph of the silicon wafer in the etching holder is presented in figure 7(*e*). Twenty membranes were processed simultaneously on a 2 inch wafer. Finally, the wafer was diced to obtain individual samples (figure 7(*f*)).

4.3.2. Point membrane deflection. The principle consists of applying a concentrated transversal load at the center of a freestanding membrane and measuring the resulting deflection. The stress value and possibly the Young's modulus of the material can be extracted from the load–deflection relationship. The stylus of a mechanical profilometer (Dektak® 150) was used to apply loads from 3 to 15 mg and measure the membrane deflection. The analytical deflection formulas for a square membrane were issued from [18, 19]. Two polyurethane membranes, with similar geometries, were analyzed. The dimensions were: side 2a = (3.36 + 0.01) mm, thickness t = (47.3 ± 0.5) μm. The Origin Pro® (8.5.1) software was used to fit the model equation to experimental data. Experimental curves were almost linear under low applied forces, as shown in figure 8, and led to an inaccurate determination of the Young's modulus: Y = (30 ± 10) MPa. Another result was the presence of a tensile stress in the

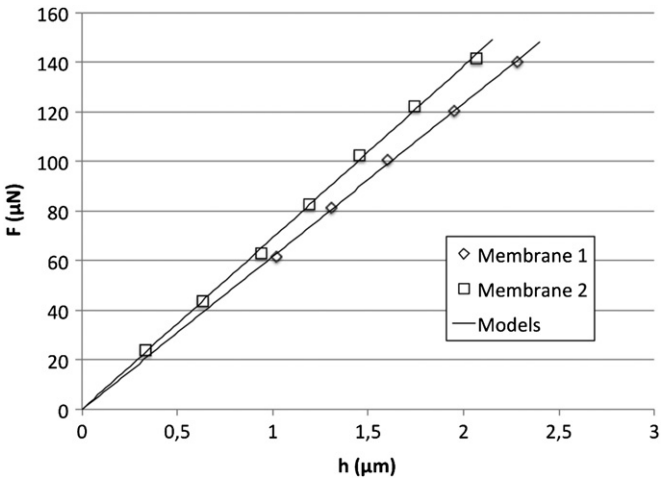

Figure 8. Load–deflection curves for two PU88 membranes.

material: σ_0 = (0.4 ± 0.1) MPa. In figure 8, the theoretical curves were obtained for a fixed stress value of 0.3 MPa. Young's modulus values of 27 MPa and 38 MPa were obtained for membranes 1 and 2, respectively, showing the effect of geometrical parameter uncertainty. Finally, those membranes were too thick to allow a precise determination of the Young's modulus. Nevertheless, the obtained values have the same order of magnitude of that resulting from tensile tests. It can be assumed that during elaboration, polyurethane films develop residual stresses. As a polyurethane film is deposited by spin-coating on a silicon substrate, a thermal stress can occur during annealing due to the mismatch of the thermal expansion coefficients of film and substrate [20]. We tried to use the bending plate method (Stoney's equation) to get a confirmation of the presence of that residual stress without success: the curvature of 4″, 150 μm thick, silicon wafers was not changed before and after polymer deposition, due to the low stiffness and the low residual stress value of the polyurethane film.

4.3.3. Pressure bulge test. The mechanical property parameters can be obtained by analyzing the mechanical response of a freestanding thin film specimen under pressurized loading. The loading versus deflection relationship for a square membrane (side length: 2a, thickness: t) was taken from [21, 22] and is given in equation (6), where P and h, stand for the applied pressure and resulting membrane center deflection, respectively. Y, ν and σ_0 are the Young's modulus, Poisson ratio and residual stress of the material, respectively. C_1 and $C_2(\nu)$ are dimensionless coefficients that depend on the membrane shape, and $C_2(\nu)$ also depends on Poisson's ratio. For a square membrane, $C_1 = 3.393$ [23]. A Poisson ratio of 0.5 was used, the corresponding $C_2(\nu)$ value was calculated as $C_2(\nu) = (0.8 + 0.062^*\nu)^{-3} = 1.74$ [24]. The displacement response was measured using a Wyko® NT1100 white-light interferometric microscope. The experimental set-up was previously detailed in [25]:

$$P = C_1 \frac{t\sigma_0}{a^2} h + C_2(\nu) \frac{t}{a^4} \frac{Y}{1-\nu} h^3 \qquad (6)$$

Table 2. Bulge test results.

Membrane	Type	a (μm)	t (μm)	σ_0 (MPa)	Y (MPa)
PU1	PU88	840 ± 50	47.4 ± 0.3	0.49 ± 0.01	28.1 ± 11.4
PU2	PU88	840 ± 50	47.7 ± 0.3	0.48 ± 0.01	20.1 ± 2.2
PU3	PU88	840 ± 50	46.8 ± 0.3	0.55 ± 0.01	22.4 ± 1.8
CB-PU	PU88 + CB	1000 ± 50	61.5 ± 0.3	0.40 ± 0.00	17.7 ± 0.2

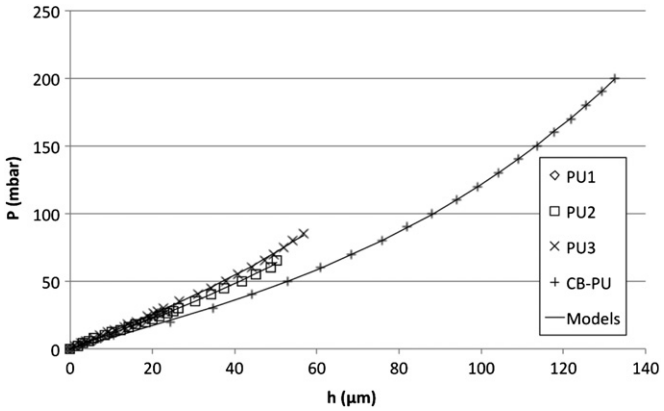

Figure 9. Pressure–deflection curves for pure and composite (carbon black) PU88 membranes.

The pressure–deflection curves for three similar pure polyurethane membranes and one composite CB-polyurethane membrane are shown in figure 9. The composite membrane was larger and thicker than pure polyurethane ones. The membrane dimensions and the best-fit residual stress and Young's modulus values are reported in table 2. The errors given for Y and σ_0 are only related to the curve-fit algorithm. These results are very similar to those obtained with the other characterization method shown previously: the Young's modulus values lie between about 10 and 30 MPa, whereas the residual stress value is about 0.5 MPa. As noted above, the determination of the Young's modulus was imprecise excepted for the composite membrane due to its lower stiffness. Finally, the presence of carbon black nanoparticles seems to have no significant influence on the Young's modulus value. But further experiments should be carried out in order to minimize measurement errors on Y.

5. Microsystem fabrication and characterization

The fabrication process for microsystems starts as membrane fabrication for the bulge test and point deflection method, but electrodes must be integrated on both faces of the PU membrane. After lift-off of the Cr/Au layer, the bottom Au electrode (40 nm) was deposited. The PU film was spin-coated. The top electrode (side length about 1.0 mm) was deposited through a mask to avoid a patterning step. Finally, the Au/PU/Au membrane was obtained after standard silicon deep etching in an aqueous KOH solution (34%, 80 °C) (figure 10(*a*)). After dicing, each sample was mounted on a T08 header and connections were made by wire-bonding. A top view of a pure PU microsystem is reported in figure 10(*b*).

The membrane was excited at its fundamental resonance frequency by applying a sinusoidal signal (electrostrictive

Table 3. MEMS characteristics.

Device	Type	a (μm)	t (μm)	f_0 (kHz)
CB-PU88-MEMS 1	PU88 + CB	840 ± 50	48.2	7.4
CB-PU88-MEMS 2	PU88 + CB	840 ± 50	48.2	7.6
PU88-MEMS 3	PU88	840 ± 50	55.0	11.2
PU88-MEMS 4	PU88	840 ± 50	55.0	8.2

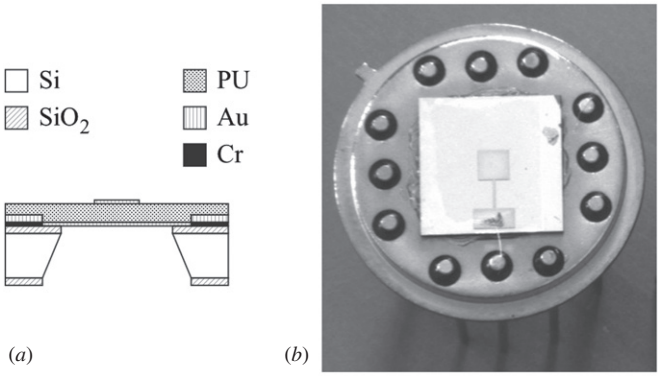

Figure 10. (*a*) MEMS schematic cross-section; (*b*) MEMS mounted on a TO8 header.

mode) from a waveform generator (Agilent® 33220A connected to a Trek® 609 D-6 voltage amplifier) to the upper electrode, with the bottom electrode held at ground potential. Another driving mode, called the pseudo-piezoelectric mode, consisted of applying a dc bias in addition to the ac excitation in order to induce permanent polarization and pre-stress the material (the dc bias voltage was chosen equal to the ac voltage amplitude). Displacements were measured at the center of the upper electrode by means of a laser vibrometer (Polytec® OFV-505 with OFV-5000 controller). The main characteristics of the microsystems are reported in table 3, where a, t and f_0 are the membrane half side length, thickness and fundamental resonance frequency, respectively. Figures 11 and 12 show the measured center deflections for pure and composite PU membranes, normalized to their thickness, as a function of the squared applied electric field. Curves are quite linear: in a first approximation, as the membrane deflection is very small compared to its thickness, the membrane has a behavior similar to that of a free film and depends on the square of the electric field, as shown in equation (3). Deflections in the pseudo-piezoelectric mode are about four times as large as those in the electrostrictive mode. It can be explained by the fact that the electric field has a constant direction in pseudo-piezoelectric mode. The induced rotation of dipoles in the material remains limited and the actuation is more efficient. Finally, deflections of composite membranes are about twice as large as those for pure PU membranes. The presence of

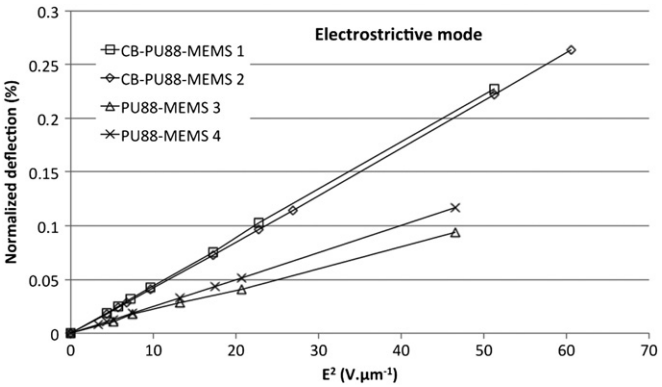

Figure 11. MEMS normalized deflection in electrostrictive mode.

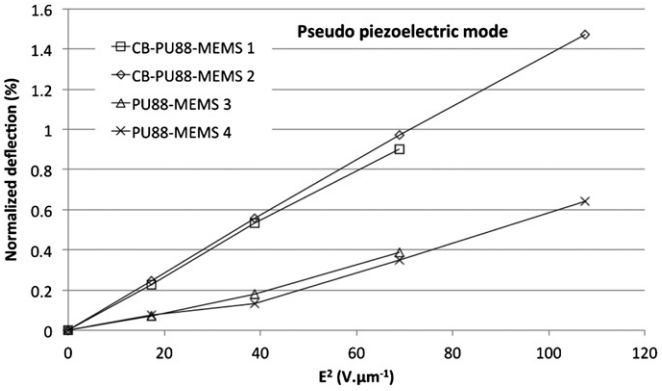

Figure 12. MEMS normalized deflection in pseudo-piezoelectric mode.

CB nanoparticles has a positive influence on the microsystem actuation. However, deflections are only limited to a few hundred nanometers because of the relatively large thickness and stiffness of the membranes. In addition, the clamping effect of the stiff metal electrodes might be important, despite their low thickness (40 nm) [26]. However, the deflections measured in this study are about one order of magnitude larger than those obtained in equivalent microsystems integrating irradiated P(VDF-TrFE) film as the membrane [27]. Another barrier to the design of PU-based actuators is related to the response time of the polymer. Beside harmonic characterizations, we also measured the voltage step-response of the microsystems and a time constant of about 800 ms was found. A value of the same order of magnitude (700 ms) was previously measured by Diaconu *et al* [6]. At the fundamental resonance frequency of the membranes, it can be assumed that the true electrostrictive effect in the material is negligible and that the membrane actuation is only due to the electrostatic interaction between the two electrodes.

6. Conclusion

The integration of carbon black nanoparticles in the polyurethane matrix has a significant influence on the dielectric permittivity of the material with an increase of about one third of its value. The Young's modulus of PU and nanocomposite PU films was determined by different characterization methods. Nanoindentation experiments have pointed out a Young's modulus gradient through the film thickness that might be related to post-deposition annealing conditions (temperature and time) and inhomogeneous solvent evaporation. By analyzing the behavior of freestanding films, an average in-plane Young's modulus value of about 30 MPa was found as well as a residual stress value of about 0.4 MPa. However, no influence of the presence of the nanoparticles was found. Finally, several MEMS actuators were realized and characterized. At their fundamental resonance frequency, the actuation of the nanocomposite membranes is more efficient than that of pure polyurethane. However, the time constant of the material seems to provide a major barrier for the development of high-frequency PU-based micro-actuators.

Acknowledgments

The authors are indebted to the institute Carnot Ingénierie@Lyon (I@L) for its support and funding, and gratefully acknowledge the facilities and technological staff from NanoLyon platform.

References

[1] Bar-Cohen Y (ed) 2004 *Electroactive Polymer (EAP) Actuators as Artificial Muscles: Reality, Potential, and Challenges* vol PM136 (Bellingham, WA: SPIE Press) p 816
[2] Shahinpoor M, Kim K J and Mojarrad M 2007 *Artificial Muscles: Applications of Advanced Polymeric Nanocomposites* (Boca Raton, FL: CRC Press, Taylor & Francis) p 387
[3] O'Halloran A, O'Malley F and Mchugh P 2008 A review on dielectric elastomer actuators, technology, applications, and challenges *J. Appl. Phys.* **104** 071101
[4] Kornbluh R, Pelrine R, Prahlad H and Heydt R 2004 Electroactive polymers: an emerging technology for MEMS *Proc. SPIE* **5344** 13–27
[5] Kim B, Park Y D, Min K H, Lee J H, Hwang S S, Hong S M, Kim B H, Kim S O and Koo C M 2011 Electric actuation of nanostructured thermoplastic elastomer gels with ultralarge electrostriction coefficients *Adv. Funct. Mater.* **21** 3242–9
[6] Diaconu I, David A and Dorohoi D-O 2005 An experimental investigation of electroactive polyurethane *J. Optoelectron. Adv. Mater.* **7** 2797–801
[7] Guillot F M and Balizer E 2003 Electrostrictive effect in polyurethanes *J. Appl. Polym. Sci.* **89** 399–404
[8] Diaconu I and Dorohoi D 2005 Properties of polyurethane thin films *J. Optoelectron. Adv. Mater.* **7** 921–4
[9] Guiffard B, Guyomar D, Seveyrat L, Chowanek Y, Bechelany M, Cornu D and Miele P 2009 Enhanced electroactive properties of polyurethane films loaded with carbon-coated SiC nanowires *J. Phys. D: Appl. Phys.* **42** 055503
[10] Wongtimnoi K, Guiffard B, Bogner-Van De Moortèle A, Seveyrat L, Gauthier C and Cavaillé J-Y 2011 Improvement of electrostrictive properties of a polyether-based polyurethane elastomer filled with conductive carbon black *Compos. Sci. Technol.* **71** 885–92
[11] Rosset S, Niklaus M, Dubois P and Shea H R 2009 Metal Ion Implantation for the fabrication of stretchable electrodes on elastomers *Adv. Funct. Mater.* **19** 470–8
[12] Ouyang G, Wang K, Henriksen L, Akram M N and Chen X Y 2010 A novel tunable grating fabricated with viscoelastic polymer (PDMS) and conductive polymer (PEDOT) *Sensors Actuators* A **158** 313–9

[13] Pimpin A, Suzuki Y and Kasagi N 2007 Microelectrostrictive actuator with large out-of-plane deformation for flow-control application *J. Microelectromech. Syst.* **16** 753–64
[14] Oliver W C and Pharr G M 2004 *J. Mater. Res.* **19** 3–20
[15] Wongtimnoi K 2011 Polyuréthanes électrostrictifs et Nanocomposites : caractérisation et analyse des mécanismes de couplages électromécaniques *PhD Dissertation* INSA Lyon, France (2011-ISAL-0152)
[16] Ignat M, Debove L and Josserond C 1996 *Bull. SMFE* **14** 10–13
[17] Malhaire C, Seguineau C, Ignat M, Josserond C, Debove L, Brida S, Desmarres J-M and Lafontan X 2009 *Rev. Sci. Instrum.* **80** 10–13
[18] Jozwik M, Delobelle P, Gorecki C, Meunier C, Munnik F, Nieradko L and Sabac A 2004 *Thin Solid Films* **468** 84–92
[19] Martins P, Delobelle P, Malhaire C, Brida S and Barbier D 2009 *Eur. Phys. J. Appl. Phys.* **45** 10501
[20] Park M-H, Jang W, Yang S-J, Shul Y and Han H 2006 Synthesis and characterization of new functional poly(urethane-imide) crosslinked networks *J. Appl. Polym. Sci.* **100** 113–23
[21] Bonnotte E, Delobelle P, Bornier L, Trolard B and Tribillon G 1997 Two interferometric methods for the mechanical characterisation of thin films by bulging test. Application to silicon single crystal *J. Mater. Res.* **12** 2234–48
[22] Maier-Schneider D, Maibach J and Obermeier E 1995 A new analytical solution for the load-deflection of square membranes *J. Microelectromech. Syst.* **4** 238–41
[23] Vlassak J J 1994 New experimental techniques and analysis methods for the study of the mechanical properties of materials in small volumes *PhD dissertation* Stanford University
[24] Vlassak J J and Nix W D 1992 A new bulge test technique for the determination of the young's modulus and the Poisson's ratio of the thin films *J. Mater. Res.* **7** 3242–9
[25] Martins P, Delobelle P, Malhaire C, Brida S and Barbier D 2009 Bulge test and AFM point deflection method, two technics for the mechanical characterisation of very low stiffness freestanding films *Eur. Phys. J. Appl. Phys.* **45** 10501
[26] Galineau J, Guiffard B, Seveyrat L, Lallart M and Guyomar D 2013 Study and modeling of an electrostrictive polyurethane diaphragm loaded with conductive carbon black *Sensors Actuators* A **189** 117–24
[27] Lam T Y, Lau S T, Chao C, Chan H L W, Choy C L, Cheung W Y and Wong S P 2007 Characterization of proton irradiated copolymer thin films for microelectromechanical system applications *Appl. Phys. Lett.* **90** 043511